ELSEVIER

Journal of Nuclear Materials 312 (2003) 266–269

journal of nuclear materials

www.elsevier.com/locate/jnucmat

Letter to the Editors

Effects of Nb content on the Zr_2Fe intermetallic stability

C. Ramos [a,*], C. Saragovi [b], M. Granovsky [a,c], D. Arias [a,c]

[a] *Instituto de Tecnología J. Sabato, CNEA-UNSAM. Av. Gral. Paz 1499, (1650), San Martín, Buenos Aires, Argentina*
[b] *Departamento de Física – CAC-Comisión Nacional de Energía Atómica. Av. Gral. Paz 1499, (1650), San Martín, Buenos Aires, Argentina*
[c] *Departamento de Materiales – CAC-Comisión Nacional de Energía Atómica. Av. Gral. Paz 1499, (1650), San Martín, Buenos Aires, Argentina*

Received 3 May 2002; accepted 13 November 2002

Abstract

With the aim of studying the stability range of the Zr_2Fe intermetallic when adding Nb, the range of existence of the cubic ternary phase (λ_1) and the corresponding two-phase field between them, four samples were analyzed, each one containing 35 at.% Fe and different at.% Nb: 0.5, 4, 10 and 15. Optical and scanning electron metallographies, X-ray diffraction, microprobe analysis and Mössbauer spectroscopy were performed to determine and characterize the phases present in the samples. Results show that the Zr_2Fe compound accepts up to nearly 0.5 at.% Nb in solution, since the $Zr_2Fe + \lambda_1$ region is stable in the (0.5–3.5) at.% Nb range. To summarize these results an 800 °C section of the ternary Zr–Nb–Fe diagram, in the studied zone, was proposed.

PACS: 81.30.Bx

1. Introduction

Zr–2.5 at.% Nb alloys are widely used in the constitutive parts of nuclear reactors of the CANDU type. Fe, which is one of the main components in steel alloys used in the reactors, is an ultra-fast diffuser in Zr and their alloys. There are also multicomponent Zr-based alloys with Sn, Nb, Fe and O, such as Zirlo (Zr–1%Nb–1%Sn–0.1%Fe–0.1%O) used as nuclear materials. All these alloys have one particularity: they present Zr–Nb–Fe precipitates [1,2]. For this reason the Zr–Nb–Fe system is of interest to the nuclear power industry.

In the revision of the binary Zr–Fe diagram Arias et al. [3] reported that the tetragonal (bct) Zr_2Fe intermetallic in the presence of a third component (O, N or C) had a cubic structure.

In earlier studies, in the ternary system Zr–Nb–Fe, we determined the presence of a cubic Ti_2Ni type phase (λ_1) [4–6].

In this work we present a further contribution to the experimental determination of the ternary phase diagram, studying the stability range of the Zr_2Fe intermetallic when adding Nb contents, the range of existence of the cubic ternary phase (λ_1) and the two phase field between them. To fulfill our objective Zr-based alloys with 35 at.% Fe and different Nb contents (0.5, 4, 10 and 15 at.%) were melted. The analysis was performed by means of optical and scanning electron microscopies (SEM), X-ray diffraction (XRD), microprobe analysis (MA) and Mössbauer spectroscopy (MS).

2. Experimental

The specimens were melted in a W electrode arc furnace in high purity argon and remelted at least three times to achieve homogeneity.

* Corresponding author. Tel.: +54-11 6772 7160; fax: +54-11 6772 7362.
E-mail address: ciramos@cnea.gov.ar (C. Ramos).

0022-3115/03/$ - see front matter
doi:10.1016/S0022-3115(02)01677-X

Samples with 0.5 and 4 at.% Nb were prepared from a Zr–2.5 at.% Nb alloy, while samples with 10 and 15 at.% Nb were made from a Zr–20 at.% Nb alloy. Both of these alloys contained $445 < \text{Fe[wt. ppm]} < 475$ and $1130 < \text{O[wt. ppm]} < 1180$. In all the cases 99.9 wt% pure Fe and 99.8 wt% pure Zr were used for the arc melting.

The ingots thus obtained were annealed at 800 °C for 1200 h, wrapped in Ta foils and sealed in silica glass in a high purity Ar atmosphere.

For metallographic analysis, sections were prepared by mechanical polishing and then chemically etched by using an adequate mixture of acids (5 vol.% HF and 5 vol.% HNO_3 twice diluted in distilled H_2O) to reveal the microstructure. Observations were performed in an optical microscope and in a scanning electron microscope (Philips PSEM 500).

The quantitative analysis was made by means of an electron microprobe (CAMECA SX 50).

Powders were prepared with a diamond-covered file in order to be used in XRD (Philips PW-1810 diffractometer) and MS (Co^{57} source in Rh matrix, at room temperature in standard transmission geometry) analysis. Mössbauer data were analyzed by superposing Lorentzian lines, applying a least squares fit procedure. Isomer shift data were given relative to αFe.

3. Results

Table 1 displays the results obtained by each one of the techniques applied. MS is used not only for identification of phases but also to describe local environments. In addition, as the area of the Mössbauer subspectra is proportional to the amount of iron compounds that produces them, it is then possible to estimate qualitatively the proportions in which each one of the phases is present in the specimens under study. Being very precise in energies, this technique is especially useful when a phase is present in a sample in a very small quantity (less than 0.1 at.%).

Own previous data [4,6], and literature research [7–9], helped us to assign the correspondent phases to the hyperfine parameters (IS, QS, BHF) shown in the table.

Table 1
Results obtained by means of X-ray diffraction, microprobe analysis and MS

Samples heat treated at 800 °C to 1200 h	Phase	Crystalline structure (XRD)	Average composition (MA) (at.%)			Mössbauer analysis			
			Zr	Nb	Fe	IS (mm/s)	QS (mm/s)	BHF (Tesla)	Area (%)
$Zr_{64.5}Nb_{0.5}Fe_{35}$	$ZrFe_2$	Cubic $MgCu_2$-type	–	–	–	−0.14	−0.02	19.55	12
	λ_1	Cubic Ti_2Ni-type	66.8	0.5	32.7	−0.13	0.31	–	22
	λ_2	–	–	–	–	−0.26	0.33	–	6
	Zr_2Fe	Tetragonal Al_2Cu-type	67.2	0.0	32.8	−0.31	0.75	–	60
$Zr_{61}Nb_4Fe_{35}$	$ZrFe_2$	Cubic $MgCu_2$-type	37.2	1.9	60.9	−0.12	0.04	17.05	23
	λ_1	Cubic Ti_2Ni-type	63.8	3.6	32.6	−0.12	0.30	–	44
	λ_2	Hexagonal $MgZn_2$-type	38.9	5.1	56.0	−0.27	0.39	–	22
	Zr_3Fe	Orthorhombic BRe_3-type	–	–	–	−0.29	0.79	–	11
$Zr_{55}Nb_{10}Fe_{35}$	λ_1	Cubic Ti_2Ni-type	58.6	8.7	32.7	−0.12	0.27	–	74
	λ_2	Hexagonal $MgZn_2$-type	36.5	20.3	43.2	−0.28	0.37	–	18
	Zr_3 Fe	–	–	–	–	−0.31	0.94	–	8
$Zr_{50}Nb_{15}Fe_{35}$	λ_1	Cubic Ti_2Ni-type	55.2	11.6	33.2	−0.14	0.25	–	77
	λ_2	Hexagonal $MgZn_2$-type	43.0	20.0	37.0	−0.30	0.31	–	15
	Zr_3Fe	–	–	–	–	−0.29	0.93	–	8

IS: isomer shift, QS: quadrupole splitting, BHF: hyperfine field. The last column values represent, in a qualitative way, the proportion in which each one of the phases is present in the correspondent sample.

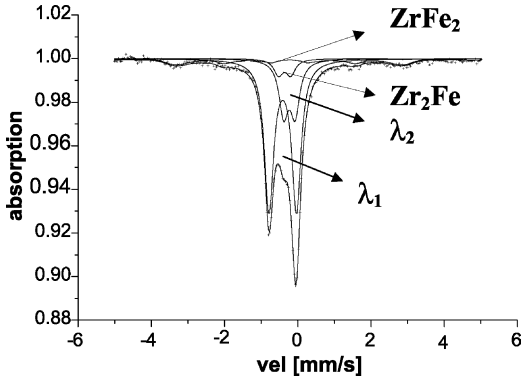

Fig. 1. Mössbauer spectrum of the $Zr_{64.5}Nb_{0.5}Fe_{35}$ sample heat-treated at 800 °C during 1200 h.

A characteristic Mössbauer spectrum of the $Zr_{64.5}Nb_{0.5}Fe_{35}$ sample heat-treated at 800 °C during 1200 h is shown in Fig. 1.

Optical microscopy and SEM analysis helped to the characterization of the samples.

4. Discussion and conclusions

In this section the results displayed in Table 1 will be discussed for each one of the phases.

4.1. Zr_2Fe and λ_1 phases

The tetragonal Zr_2Fe compound was only found in the $Zr_{64.5}Nb_{0.5}Fe_{35}$ sample, while the λ_1 phase was present in all of the samples.

We have already reported [4–6], the formation of a cubic ternary phase (λ_1) from the Zr_2Fe intermetallic with Nb content.

In fact, in Table 1 (see MA results), Nb in λ_1 phase increases at the expense of Zr at the same time as Nb increases in the samples (Fe remaining around 32 at.%). This assumption supports the differences in the observed hyperfine parameters obtained by MS [4].

The results mentioned above allow to conclude that the at.% Nb boundary between Zr_2Fe and λ_1 phases is approximately 0.5 at.%. MA analysis also showed that the $Zr_2Fe + \lambda_1$ region would be stable in the (0.5–3.5) at.% Nb range.

Likewise it is interesting to observe that the proportion of λ_1 phase increases when the at.% Nb increases in the respective samples.

4.2. $ZrFe_2$ phase

The $ZrFe_2$ intermetallic, with cubic Laves $MgCu_2$-type structure (C15) was present in the $Zr_{64.5}Nb_{0.5}Fe_{35}$ and $Zr_{61}Nb_4Fe_{35}$ samples.

Mössbauer analysis gave a six-line pattern due to this ferromagnetic compound. It was fitted with a distribution of hyperfine fields considering that Fe surroundings are slightly different. In Table 1 the maximum probability hyperfine fields are displayed.

The values of BHF found, which are different to that reported in literature [7] (~20 T for the binary compound), indicate local modification of the $ZrFe_2$ structure; the lower values suggest the substitution of Fe or Zr atoms by the non-magnetic Nb atoms meanwhile the higher values suggest Fe-rich surroundings.

MA results for this phase in the $Zr_{64.5}Nb_{0.5}Fe_{35}$ sample are not displayed in Table 1 because measurements were not accurate due to the morphology of the phase in this sample. It appeared scarcely and as very small precipitates, then covering the microprobe beam a volume of about 1 μm^3, we were also measuring part of the matrix phase. Fe/Nb ratios were calculated but the scarce quantity of these precipitates in this sample did no allow a good statistic.

The limit shown for the Zr_2Fe phase in the proposed diagram at 800 °C (Fig. 2) was determined in [8].

4.3. λ_2 phase

Granovsky et al. [5] studying samples which cover the following range: $41 < Zr < 97$, $0.9 < Nb < 32$, $0.6 < Fe < 38$, detected a ternary phase $(Fe + Nb)_2Zr$ and indexed it as the hexagonal Laves phase $MgZn_2$ type (C14) structure by means of XRD.

In our case by means of MA we detected a phase (denominated λ_2) with a wide range of compositions, $37 < Fe$ (at.%) < 56, accepting Nb contents up to 20 at.%. This hexagonal Laves $MgZn_2$-type phase was identified in the $Zr_{61}Nb_4Fe_{35}$, $Zr_{55}Nb_{10}Fe_{35}$ and $Zr_{50}Nb_{15}Fe_{35}$ samples by XRD. For the latter sample the lattice parameters that we found are: $a = 0.523$ nm and $c = 0.850$ nm. In the $Zr_{64.5}Nb_{0.5}Fe_{35}$ sample XRD analysis was inconclusive.

MS results confirmed the presence of this C14-type phase, [9]. The hyperfine parameters could be determined fixing the Mössbauer parameters of all the other phases. The values thus obtained are supported by our previous work [6]. The wide range of compositions it admits produces different values for the corresponding QS.

This result does not argue with other studies [2] that inform the presence of precipitates of hexagonal crystalline structure in a wide range of compositions in the central region of the Zr–Nb–Fe diagram.

The $Zr_{64.5}Nb_{0.5}Fe_{35}$ sample only has traces of this phase presumably owing to inhomogeneities during casting. We assume that λ_2 presence is due to the slow dissolution at 800 °C. This behavior suggests that the Zr, Nb and Fe diffusion coefficients are low in this inter-

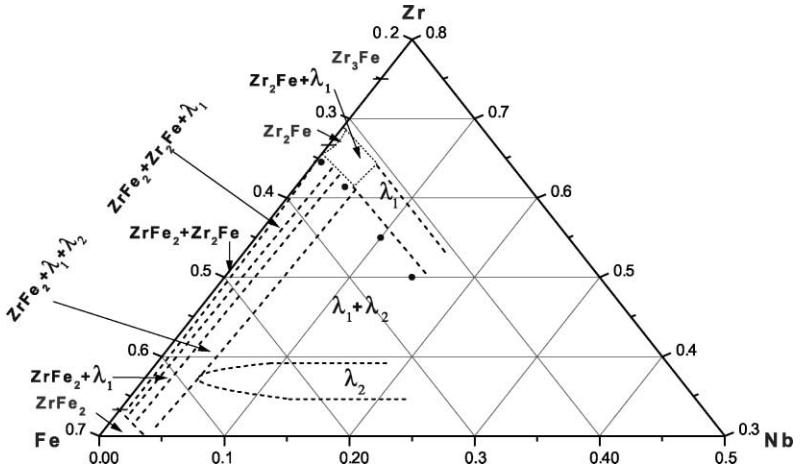

Fig. 2. Isothermal section proposed at 800 °C: (•) studied compositions, (- - -): probable, (. . .) predicted.

metallic phase, as it is rather usual in the intermetallic diffusion process. Therefore, for this sample, the λ_2 phase will not be considered in the proposed section of the diagram at 800 °C (Fig. 2).

4.4. Zr_3Fe phase

Traces of this orthorhombic phase are suggested taking into account the MS areas, which indicate their minor proportion in all of the samples. These traces are presumably due to small inhomogeneities caused in the material during casting and they could have been eliminated with a longer heat treatment, probably at higher temperature. Because of this, Zr_3Fe traces will not be considered when proposing the corresponding fields in the phase diagram (Fig. 2).

Mössbauer parameters in literature [10] show that Zr_2Fe and Zr_3Fe phases exhibit the same IS and similar QS values in the binary system Zr–Fe. However our previous studies in the ternary system Zr–Nb–Fe [4], show that the Nb content modify the QS values for the Zr_3Fe phase, remaining the IS equal to that of Zr_2Fe. In this case all of the other techniques are useful to distinguish between Zr_2Fe and Zr_3Fe in the ternary system.

In concluding, the present results together with those from Granovsky et al. [5] allow us to propose the isothermal section (800 °C) displayed in Fig. 2, in which both the probable and predicted fields are clearly pointed out.

References

[1] V.A. Markelov, V.Z. Ratikov, S.A. Nikulin, V.I. Goncharov, V.N. Shishov, A.Yu. Gusev, E.K. Chesnokov, Phys. Met. Metall. 77 (1994) 380.
[2] V.N. Shishov, A.V. Nikulina, V.A. Markelov, M.M. Peregud, A. Kozlov, S. Averin, S. Kolbenkov, A. Novoselov, in: Proceedings of the 11th Int. Symp. on Zr in the Nuclear Industry, ASTM STP, Vol. 1295, 1996, p. 603.
[3] D. Arias, M.S. Granovsky, J.P. Abriata, in: H. Okamoto (Ed.), Phase Diagrams of Binary Iron Alloys, ASM International Materials, Metals Park, OH, 1993.
[4] C. Ramos, C. Saragovi, M. Granovsky, D. Arias, Hyperfine Interact. 122 (1999) 201.
[5] M.S. Granovsky, M. Canay, E. Lena, D. Arias, J. Nucl. Mater. 302 (2002) 1.
[6] C. Ramos, C. Saragovi, M. Granovsky, D. Arias, Hyperfine Interactions 139 (1) (2002) 363.
[7] F. Labenski de Kanter, C. Saragovi Badler, M. Granovsky, D. Arias, Applications of the Mössbauer Effect, World Scientific, Singapore, 1992, p. 246.
[8] Z. Kanematsu, J. Phys. Soc. Jpn. 27 (4) (1969) 849.
[9] A.W. Smith, R.D. Rawlings, Phys. Stat. Sol. (A) 22 (1974) 491.
[10] F. Aubertin, U. Gonser, S.J. Campbell, H.G. Wagner, Z. Metall. 76 (4) (1985) 237.